ELSEVIER

Chemical Engineering Journal 137 (2008) 308–319

Chemical Engineering Journal

www.elsevier.com/locate/cej

Kinetic modeling of liquid phase autoxidation of cumene

Arijit Bhattacharya *

Chemical Engineering and Process Development Division, National Chemical Laboratory, Pune 411008, India

Received 25 January 2007; received in revised form 26 April 2007; accepted 26 April 2007

Abstract

A new kinetic model for the liquid phase autoxidation of cumene has been developed utilizing the existing knowledge about the traditional free-radical mechanism involving the initiation of the free-radicals, the chain propagation and transfer and the various modes of radical termination. Unlike previous work, in the re-organized reaction network an important cross-termination step replaces an often used but less likely one and a new derivation of the rate model has been provided. A base set of rate parameters for the elementary steps within this reaction network were chosen, many of them were same or very similar to those published in the literature, with a few critical ones re-estimated for correct match with directly observed kinetic data reported in the literature on cumene oxidation in bench scale reactors. Embedding this kinetic sub-model within a simple reaction engineering model for a single air-sparged continuous cumene oxidator, the liquid oxidate composition at the reactor exit could be predicted that compared closely with some limited published data from an industrial reactor. It is hoped that the kinetic model presented here would be a useful tool in the analysis and design of other autoxidation reactors as well with minor adaptations.

Keywords: Liquid phase autoxidation; Cumene oxidation; Free-radical mechanism; Kinetic model; Air-sparged continuous oxidator

1. Introduction

Liquid phase oxidation (LPO) of hydrocarbons using air or oxygen as the oxidant is a unit process that provides an efficient and practical means of producing in very large scale many organic chemical intermediates of importance to the petrochemical industry [1–3]. Some important examples are air oxidation of cyclohexane to cyclohexanol and cyclohexanone enroute to adipic acid, that of cumene to cumene hydroperoxide as a precursor to phenol, those of *p*-xylene to terephthalic acid, isobutane to *tert*-butyl hydroperoxide, etc. More recently, liquid phase oxidation of cycloalkenes have been categorized [3] as among the significant emerging LPO processes that may provide, in the near future, alternative routes to cyclohexanol, cyclohexanone, cyclohexene epoxide, cyclododecanone, cyclododecene epoxide and a host of other useful intermediates.

Initial formation of a reactive hydroperoxide from the hydrocarbon concerned appears as a common pathway in the above LPO processes, which is followed by further transformations of the hydroperoxide catalytically or otherwise to stable products like alcohols and ketones in situ. Generally speaking, presence of metal complexes and/or strong acids catalyzes the hydroperoxide decomposition.

Production of cumene hydroperoxide (CHP), which is among the very few examples of large-scale manufacture of a stable hydroperoxide product, naturally uses an uncatalyzed LPO process operated at about 105–115 °C and 6–7 bar [4]. The conversion is limited to about 22–25% in order to limit the build up of the side products like dimethylphenylcarbinol (DMPC) and acetophenone (ACP) produced by decomposition of the primary product, i.e., CHP. The oxidation process is conducted in a set of four to six serially connected bubble column reactors in order to improve the selectivity. Cumene hydroperoxide is cleaved to acetone and phenol by a different unit process in a subsequent section of a standard phenol plant based on the Hock process. Apart from the major side products mentioned above some acids, like formic acid, are also formed in the oxidate that would accentuate the decomposition of CHP and result in the loss of selectivity. Small quantities of aqueous carbonate–bicarbonate buffer solutions are injected to the reactor to neutralize the acids. In more recent installations these additions are said to be minimized, higher reactor temperatures, 130–140 °C, are used, up to 30% hydrocarbon conversion allowed [3]. Continuing improvement of the efficiency and the

* Tel.: +91 20 2590 2166; fax: +91 20 2590 2612.
E-mail address: a.bhattacharya@ncl.res.in.

1385-8947/$ – see front matter © 2007 Elsevier B.V. All rights reserved.
doi:10.1016/j.cej.2007.04.043

Nomenclature

a'	specific interfacial area for solid–liquid mass transfer (m^{-1})
A	frequency factor (s^{-1} or m^3/kmol/s)
C	concentration of the liquid phase components (kmol/m^3)
E	activation energy (kJ/mol)
H	Henry's law constant (MPa m^3/kmol)
k	rate constants for the elementary reactions (m^3/kmol/s)
k_l	gas–liquid mass transfer coefficient (m/s)
K	combined rate constant as defined by Eq. (19)
N_R	number of reactor stages
OX	oxygen
p_{O_2}	oxygen partial pressure (MPa)
p'_{O_2}	partial pressure of oxygen in equilibrium with the dissolved oxygen concentration (MPa)
R	rate of consumption/production of a liquid phase species (kmol/m^3/s)
RH	cumene
ROOH	cumene hydroperoxide
t	time (s)
u_g	superficial air velocity (m/s)

Greek letter

ε_g	gas hold-up

Subscript

j	component

Superscript

o	initial

profitability of the process critically depends on better understanding of the process kinetics and improved specification and control of the operating conditions.

There have been a considerable number of studies on the mechanism and the kinetics of homogeneous liquid phase uncatalyzed oxidation (or 'autoxidation') of hydrocarbons, the early work being summarized in the much-cited treatise by the Russian scientists [5]. Since then the basic framework of free-radical mechanism underlying the LPO processes has been generally established. The kinetics of individual elementary reaction steps that constitute the overall reaction network, like propagation, chain transfer and termination, have been extensively studied using a variety of model hydrocarbon species. This body of work can be accessed from a number of reviews and monographs [6–9]. Attention had also been specifically devoted to the mechanism and kinetics of autoxidation of cumene [10,11].

A pioneering study made by Hattori et al. [12] on the kinetics of cumene oxidation in a laboratory bubble column represented an early adaptation by chemical engineers of the broad free-radical mechanistic framework to the rate analysis. They also presented a classic derivation of a simplified expression for the overall rate of CHP production that had been used with minor modifications much later by Andrigo et al. [13] in their study of kinetics of cumene oxidation in a CSTR ('micropilot reactor') and in their simulation of the performance of an industrial scale reactor. It is fairly common to find essentially the same or very similar rate expressions quoted in more recent literature as well [14,15] in respect of liquid phase air oxidation of hydrocarbons in general.

Suresh et al. [16] have examined the kinetics of the uncatalyzed LPO of cyclohexane, conducted in a stainless steel semi-batch reactor (with continuous flow of diluted air). In order to interpret the apparent autocatalytic behaviour observed in their experimental data on the rate of oxygen absorption and dissolved oxygen concentration, they proposed a closed form kinetic model based on simplification of the classical free-radical scheme by lumping all manner of products into one. There was no way to identify the net rates of formation of the key products such as cyclohexanol and cyclohexanone nor the side product acids.

To interpret their laboratory kinetic data on the catalyzed (e.g. with cobalt naphthenate as the catalyst) oxidation of cyclohexane, Pohorecki et al. [17] had postulated a reaction network comprising of a rather eclectic admixture of some elementary free-radical steps and some molecular lumped reactions assumed to account for the generation of the byproduct(s). The fundamental structure of the free-radicals based reaction network, could not be retained partly because of the admitted need to modify a more empirically derived scheme depending on the kind of catalysts used.

In an earlier publication from our group we had shown [18], in the context of the uncatalyzed liquid phase oxidation of cyclohexane, that one could come up with a more general treatment of the appropriate free-radical kinetics without any lumping of species and at the same time without making the assumptions inherent in Hattori et al.'s treatment [12]. On that basis it was possible for us to derive the pertinent component rates and selectivity and allowed us to predict Suresh et al.'s data [16] on the rate of oxygen absorption and dissolved oxygen concentration.

In the present work, we first present a consistent free-radical mechanism comprising of most of the proposed elementary steps, which are known to be significant, in the case of cumene autoxidation, but with some re-organization and re-emphasis. This is to be followed by a general kinetic analysis based on such a network without having recourse to some simplifying assumptions routinely made by the previous workers. All the component rates especially those of cumene depletion, oxygen consumption and the CHP production would be derived based on this kinetic model and used for prediction of the performance of a batch oxidation reactor. By a critical review of the information and data available in the literature on the free-radical kinetics pertinent to liquid phase autoxidation reactions and some directly observed kinetic data [12,13] on cumene oxidation in bench scale reactors, appropriate values will be assigned to all the necessary rate parameters in the model.

Finally, for a continuous air-sparged oxidator, much like the ones used in commercial installations, an attempt will be made to devise a simple model, with the embedded kinetic sub-model as developed here, for predicting the liquid oxidate composition

at the exit of the reactor. It would be interesting to see how well do these predictions compare with the limited reported data from the literature.

2. Previous work on cumene autoxidation modeling

On the basis of the state of knowledge on the free-radical mechanism for the homogeneous liquid phase autoxidation of hydrocarbons, as summarized by Emanuel et al. [5], Hattori et al. [12] proposed a reaction network for cumene autoxidation that has remained basic to the subsequent developments. They suggested a possible set of initiation reactions such as generating alkyl radicals either by direct decomposition or dehydrogenation of cumene or by the reaction of the latter with initiator radicals produced in situ. While these pathways may cause the initial formation of cumene hydroperoxide (CHP) in marginal quantities, it is generally agreed that radical generation by the decomposition of CHP followed by further reaction with the hydrocarbon is probably the more significant mode of initiation:

$$ROOH \rightarrow RO^{\bullet} + {}^{\bullet}OH \quad (I)$$

$${}^{\bullet}OH + RH \rightarrow R^{\bullet} + H_2O \quad (II)$$

$$RO^{\bullet} + RH \rightarrow R^{\bullet} + ROH \quad (III)$$

Direct addition of dioxygen to the cumyl radicals to produce the cumyl peroxy radicals followed by the hydrogen abstraction by the latter from cumene producing CHP constituted, in Hattori et al.'s scheme, the propagation steps:

$$R^{\bullet} + O_2 \rightarrow RO_2^{\bullet} \quad (IV)$$

$$RO_2^{\bullet} + RH \rightarrow R^{\bullet} + ROOH \quad (V)$$

They considered two basic types of bimolecular termination reactions, namely, the self-terminations involving either $R^{\bullet}$ or $RO_2^{\bullet}$ and the cross-termination between $R^{\bullet}$ and $RO_2^{\bullet}$:

$$2R^{\bullet} \rightarrow RR \quad (VI)$$

$$R^{\bullet} + RO_2^{\bullet} \rightarrow ROOR \quad (VII)$$

$$2RO_2^{\bullet} \rightarrow ROOR + O_2 \quad (VIII)$$

where R in the termination products RR and ROOR is usually derived from the cumyl radical, though other competing alkyl radicals, if and when present, may sometimes contribute.

Though Hattori et al. concerned themselves essentially with the rates of CHP production and cumene and oxygen consumption, their scheme indicated, at least formally, pathways to produce the alcohol (DMPC), as in step (III), and the ketone (ACP), as in step (IX) (the so-called β-cleavage [8]):

$$RO^{\bullet} \rightarrow 2Ph\,C(O)CH_3 + CH_3^{\bullet} \quad (IX)$$

Andrigo et al. [13] took the above framework as their point of departure and enriched the network further by including additional elementary steps (notably some important chain transfer and termination steps, such as the self-reaction of the peroxy radical, $RO_2^{\bullet}$, to form the alkoxy radical $RO^{\bullet}$ and the cross-termination between the methyl peroxy and cumyl peroxy radicals) in the light of further advances [8,10] in the knowledge base on the cumene autoxidation kinetics. This constituted a significant progress in the mechanism development that could account for not only the primary product CHP and the main byproducts DMPC, ACP and ROOR in the oxidate, but also minor critical side products like formic acid. This latter part of the scheme involved the formation, the propagation and the termination of the methyl peroxy radical:

$$CH_3^{\bullet} + O_2 \rightarrow CH_3O_2^{\bullet} \quad (X)$$

$$CH_3O_2^{\bullet} + RH \rightarrow CH_3OOH + R^{\bullet} \quad (XI)$$

$$CH_3O_2^{\bullet} + RO_2^{\bullet} \rightarrow HCHO + ROH + O_2 \quad (XII)$$

$$HCHO + 0.5O_2 \rightarrow HCOOH \quad (XIII)$$

However, while the reaction scheme due to Andrigo et al. presented in their Fig. 1 [13] appears exhaustive, the scheme listed far too many elementary steps, one is afraid in a somewhat eclectic manner, some of which may not be as important as others from the theoretical and the kinetic considerations. Kinetic analysis involving all these reactions in a general manner would be very complicated and parameter estimation unwieldy. On the other hand, the importance of certain key chain transfer and termination reactions seem to have been lost in their being relegated to *secondary side reaction* steps. In this work, we propose to make the reaction network both compact and more consistent with the available and pertinent information in the literature.

Having assumed a reaction network comprising of the elementary steps (I) through (VIII), Hattori et al. [12] proceeded in a classical manner (assuming a pseudo-steady state with respect to the concentration of the radicals $RO^{\bullet}$, $R^{\bullet}$ and $RO_2^{\bullet}$) to derive closed form equations for the rate of cumene depletion and that of CHP production. These calculated rates compared fairly well with the limited experimental rate data generated by the authors. But in their derivation they made two assumptions, namely, that $2\sqrt{k_{VI}k_{VIII}} = k_{VII}$ and $k_{VI} = k_{VIII}$. It is generally believed [8–10] that except under conditions where dissolved oxygen concentration is drastically depleted (which is rarely the condition characterizing a well-designed and operated oxidator in practice), it is the step (VIII) that would be the dominant termination mode. It is possible to argue that to cover the eventuality of a very highly mass transfer controlled and/or otherwise oxygen starved condition, occurrence of the self-termination among the $R^{\bullet}$ radicals or even the cross-termination between $R^{\bullet}$ and $RO_2^{\bullet}$ radicals might be needed. The particular assumptions by Hattori et al. [12], however, appear to have been made mainly to simplify their derivation. We did not find any data or other evidence in the pertinent literature [6–11] supporting these very specific relationships between the various termination rate constants.

While the probability of occurrence of the cross-termination between $R^{\bullet}$ and $RO_2^{\bullet}$ (step (VII)) may indeed be low, that between methyl peroxy and cumyl peroxy radicals (step (XII)) may be much more significant, which was quite convincingly argued and demonstrated [11] by some systematic and well-designed experiments. This would suggest that there might be a case for including step (XII) as a parallel and perhaps the dominant cross-termination step in the overall reaction network. The

above assumptions, pivotal to the development of the fundamental rate equations due to Hattori et al. [12] would be invalid in such a case.

Andrigo et al. [13] by making the same assumptions as Hattori et al. [12], obtained essentially the same rate equation for CHP as in Ref. [12]. They then extended similar methodology to the elementary steps around the methyl radical. There is a need to free the treatment of the kinetics of cumene autoxidation from the legacy of the assumptions such as above that does not seem to have any factual basis. This would presage the development of a more general methodology that could apply to kinetic modeling of other traditional LPO processes [16] as well as the emerging ones [19,20] as well. As we shall show later in the paper, a general kinetic analysis can be successfully made without assuming such relationships.

3. New kinetic model

3.1. Model equations

Based on a careful study of the previous work on the kinetic modeling of cumene autoxidation, we present below the complete set of elementary reactions forming the overall reaction network.

$$\mathrm{ROOH} \xrightarrow{k_1} \mathrm{RO^\bullet} + {}^\bullet\mathrm{OH}$$

$${}^\bullet\mathrm{OH} + \mathrm{RH} \xrightarrow{k_2} \mathrm{H_2O} + \mathrm{R^\bullet}$$

$$\mathrm{R^\bullet} + \mathrm{O_2} \xrightarrow{k_3} \mathrm{RO_2^\bullet}$$

$$\mathrm{RO_2^\bullet} + \mathrm{RH} \xrightarrow{k_4} \mathrm{ROOH} + \mathrm{R^\bullet}$$

$$\mathrm{RO^\bullet} + \mathrm{RH} \xrightarrow{k_5} \mathrm{ROH} + \mathrm{R^\bullet}$$

$$\mathrm{RO^\bullet} + \mathrm{ROOH} \xrightarrow{k_6} \mathrm{ROH} + \mathrm{RO_2^\bullet}$$

$$2\mathrm{RO_2^\bullet} \xrightarrow{k_7} \mathrm{O_2} + 2\mathrm{RO^\bullet}$$

$$\mathrm{RO^\bullet} \xrightarrow{k_8} \mathrm{Ph\,C(O)CH_3} + \mathrm{CH_3^\bullet}$$

$$\mathrm{CH_3^\bullet} + \mathrm{O_2} \xrightarrow{k_9} \mathrm{CH_3O_2^\bullet}$$

$$\mathrm{CH_3O_2^\bullet} + \mathrm{RH} \xrightarrow{k_{10}} \mathrm{CH_3OOH} + \mathrm{R^\bullet}$$

$$\mathrm{R^\bullet} + \mathrm{RO_2^\bullet} \xrightarrow{k_{11}} \mathrm{ROOR}$$

$$\mathrm{CH_3O_2^\bullet} + \mathrm{RO_2^\bullet} \xrightarrow{k_{12}} \mathrm{ROH} + \mathrm{HC(O)H} + \mathrm{O_2}$$

$$2\mathrm{RO_2^\bullet} \xrightarrow{k_{13}} \mathrm{O_2} + \mathrm{ROOR}$$

$$2\mathrm{R^\bullet} \xrightarrow{k_{14}} \mathrm{RR}$$

It will be noticed that the above network adequately and concisely manifests all the important mechanistic pathways reported in the pertinent literature [8–13], while pruning others that, in our judgment, would not contribute materially to either the overall component rates or the product distribution usually observed in commercial plant operations [4,13]. For the sake of completeness we have included in the above scheme the cross-termination between $\mathrm{R^\bullet}$ and $\mathrm{RO_2^\bullet}$ radicals. However, in view of what has been said in the previous section on the relatively more important cross-termination between the methyl peroxy and the cumyl peroxy radicals, the former termination step (step 11 in the above scheme) has been ignored in deriving the rate equations as summarized below. The corresponding equations including this step is equally easy to derive, but will not be presented here.

Given the above scheme, writing the equations for the rate of accumulation of the radicals, ${}^\bullet\mathrm{OH}$, $\mathrm{CH_3^\bullet}$, $\mathrm{CH_3O_2^\bullet}$, $\mathrm{RO^\bullet}$, $\mathrm{R^\bullet}$, $\mathrm{RO_2^\bullet}$, equating these rates to zero in view of the quasi-steady state assumption with reference to each of these species, and solving for the corresponding concentrations would result in the following equations:

$$[{}^\bullet\mathrm{OH}] = \frac{k_1[\mathrm{ROOH}]}{k_2[\mathrm{RH}]} \tag{1}$$

$$[\mathrm{CH_3^\bullet}] = \frac{k_8[\mathrm{RO^\bullet}]}{k_9[\mathrm{OX}]} \tag{2}$$

$$[\mathrm{CH_3O_2^\bullet}] = \frac{2k_8[\mathrm{RO^\bullet}]}{k_{10}[\mathrm{RH}] + k_{12}[\mathrm{RO_2^\bullet}]} \tag{3}$$

$$[\mathrm{RO^\bullet}] = \frac{4k_1[\mathrm{ROOH}] + 2k_7[\mathrm{RO_2^\bullet}]^2}{2k_8 + k_5[\mathrm{RH}] + 3k_6[\mathrm{ROOH}]} \tag{4}$$

$$[\mathrm{R^\bullet}] = \frac{-\mathrm{BB} + \sqrt{\mathrm{BB}^2 - 4(\mathrm{AA})(\mathrm{CC})}}{2(\mathrm{AA})} \tag{5}$$

where $\mathrm{AA} = 4k_{14}$, $\mathrm{BB} = 3k_3[\mathrm{OX}]$ and $\mathrm{CC} = -\left[4k_1[\mathrm{ROOH}] + k_4[\mathrm{RO_2^\bullet}][\mathrm{RH}] + \left\{k_5 + \frac{2k_8k_{10}}{k_{10}[\mathrm{RH}+k_{12}[\mathrm{RO_2^\bullet}]}\right\}[\mathrm{RO^\bullet}][\mathrm{RH}]\right]$.

The concentration of the $\mathrm{RO_2^\bullet}$ radicals would be calculated by solving the following equation:

$$3k_3[\mathrm{R^\bullet}][\mathrm{OX}] - 2(k_7 + k_{13})[\mathrm{RO_2^\bullet}]^2 - k_4[\mathrm{RO_2^\bullet}][\mathrm{RH}] + 3k_6[\mathrm{RO^\bullet}][\mathrm{ROOH}] - \frac{2k_8k_{12}[\mathrm{RO^\bullet}][\mathrm{RO_2^\bullet}]}{k_{10}[\mathrm{RH}] + k_{12}[\mathrm{RO_2^\bullet}]} = 0 \tag{6}$$

The equations to calculate the net rates of consumption/production of various molecular reactant or product species by all the concerned reaction steps can then be written as follows:

Oxygen

$$R_{\mathrm{OX}} = -3k_3[\mathrm{OX}][\mathrm{R^\bullet}] + (k_7 + k_{13})[\mathrm{RO_2^\bullet}]^2 - 2k_8[\mathrm{RO^\bullet}] + \frac{2k_8k_{12}[\mathrm{RO^\bullet}][\mathrm{RO_2^\bullet}]}{k_{10}[\mathrm{RH}] + k_{12}[\mathrm{RO_2^\bullet}]} \tag{7}$$

Cumene

$$R_{RH} = -4k_1[ROOH] - [RH]\left[k_4[RO_2^\bullet] + \left\{k_5 + \frac{2k_8k_{10}}{k_{10}[RH] + k_{12}[RO_2^\bullet]}\right\}[RO^\bullet]\right] \quad (8)$$

CHP

$$R_{CHP} = -4k_1[ROOH] + k_4[RH][RO_2^\bullet] - 3k_6[ROOH][RO^\bullet] \quad (9)$$

DMPC

$$R_{DMPC} = [RO^\bullet]\{k_5[RH] + 3k_6[ROOH]\} + \frac{2k_8k_{12}[RO^\bullet][RO_2^\bullet]}{k_{10}[RH] + k_{12}[RO_2^\bullet]} \quad (10)$$

ACP

$$R_{ACP} = 2k_8[RO^\bullet] \quad (11)$$

ROOR

$$R_{ROOR} = k_{13}[RO_2^\bullet]^2 \quad (12)$$

RR

$$R_{RR} = 2k_{14}[R^\bullet]^2 \quad (13)$$

In order to test the above kinetic model by comparing calculated results against observed integral kinetic data (such as the ones presented by Hattori et al. [12]) one has to write and solve the following batch reactor equations for the concentration of the seven species as above.

Oxygen

$$\frac{d[OX]}{dt} = R_{OX} + \frac{k_l a'}{1-\varepsilon_g}\left(\frac{p_{O_2}}{H} - [OX]\right) \quad (14)$$

Other species

$$\frac{d[C]_j}{dt} = R_j \quad (15)$$

with the subscript j varying from 2 through 7 denoting cumene, CHP, DMPC, ACP, ROOR and RR, respectively. The equations are subject to the following initial conditions:

$$[OX] = 0, \quad [RH] = [RH]^o, \quad [C]_j = 0, \quad j = 3-7 \quad (16)$$

The above equations were written with the following assumptions:

- isothermal operation;
- homogeneous liquid phase;
- negligible vapour pressure for the liquid reactant and the product species;
- gas phase (air or diluted air) maintained at a constant pressure;
- oxygen mass transfer resistance essentially in the liquid phase.

The equations would be applicable, in general, to traditional experiments where the reactor is operated with air or oxygen flowing in and out of a semi-batch bubble column [12] or an agitated sparged reactor [16]. As assumed and *a posteriori* justified by Hattori et al. [12] in the former case, a quasi-steady state with respect to the dissolved oxygen concentration under the so-called 'slow reaction regime' operation may obtain in the reactor. It is, in general, appropriate to solve the dynamic Eq. (14) along with the others (as it was done by Bhattacharya and Mungikar [18]) and allow the dissolved oxygen concentration to find and reach eventually an approximately invariant level.

The model would also be applicable with minor modifications to the typical experimental protocol used in many recent LPO kinetic studies [19,20]. In these experiments usually oxygen flows into a batch of liquid reactant, kept at a constant temperature, from a reservoir through a constant pressure regulator. There is no gas flow out. Thus, the net flow of oxygen into the reactor provides the rate of oxygen absorption.

3.2. Solution procedure

Eq. (14) and those represented compactly by Eq. (15), subject to Eq. (16) were solved in this work by using the IMSL ODE solver IVPAG. The rate expressions for R_j were obtained using Eqs. (7) through (13) and the required concentrations of the radicals were evaluated using Eqs. (1) through (6). Before solving such a set of equations to obtain the temporal profiles of the various species concentrations, one needs to assign or estimate values for a number of parameters. A discussion on how this was done is in order.

The value of Henry's law constant for oxygen was found using the published data on the oxygen solubility in cumene [21], which was also reported to be fairly insensitive to temperature. The mass transfer coefficient k_l, gas hold-up ε_g and the specific interfacial area a' were calculated by using the Akita–Yoshida correlation [22], taking the physicochemical properties for a liquid phase composition corresponding to about 30% conversion of cumene (liquid phase comprising of a mixture of cumene and CHP). The calculated values of these parameters at 120 °C are summarized in Table 1. The calculated value of the mass transfer coefficient turned out to be very close to what was experimentally determined by Hattori et al. [12]. The two other parameter values are also in the expected range.

The key to successful kinetic modeling of the autoxidation, however, is the correct assignment of the values to the large number of kinetic parameters (13, to be exact, at any temperature level, and double this number if we are to consider data at different temperatures). A full-fledged parameter estimation work given extensive integral kinetic data is possible, though it is not an easy task. Andrigo et al. [13] claimed to have made such

Table 1
Estimated values of the hydrodynamic and mass transfer parameters for the cumene autoxidation experiments [12]

Parameters	Values
Liquid side mass transfer coefficient (k_l)	9.38×10^{-4} m/s
Interfacial area (a')	141.4 m^{-1}
Volumetric mass transfer coefficient ($k_l a'$)	0.13 s^{-1}
Gas hold-up (ε_g)	8.68×10^{-2}

an attempt with the performance data generated in their pilot scale CSTR. However, the kinetic constants were not reported, nor the complete set of data. The limited integral kinetic data presented by Hattori et al. [12] would not suffice to estimate such a large number of parameters. Instead of values for individual rate constants, Hattori et al. [12] came up with lumping of several rate constants (for the propagation and the termination) quite in line with similar combinations one finds in the classical literature on the kinetics of free-radicals based reactions. In this work, we chose a slightly different approach.

There exists extensive literature data [8–11] on the measured or estimated values of the rate constants for most classes of elementary reactions of importance in autoxidation (sometimes for cumene itself and at other times for other similar model hydrocarbons). In view of this, one was prompted to examine the reliability of the values of these constants, if required reassign values to them in the light of the observed kinetic data [12,13]. Table 2 summarises suggested values (at 120 °C) for the nine rate constants that one obtains from the perusal of the literature. This includes the rate constants for all the propagation and transfer reactions and those for the key initiation and the bimolecular self-termination reaction of the $RO_2^\bullet$ radicals (step 13). Rate constants for the steps 2 and 9 are not important as the rates for these steps could be replaced, in the above analysis, in terms of those for the adjacent initiation and the propagation steps, respectively. That leaves the rate constants for the cross-termination step 12 and the self-termination of the $R^\bullet$ radicals (step 14) to be estimated, apart from reassigning values to the other nine rate constants as above so as to closely approximate a given set of rate data.

Table 3 summarises the values of the frequency factor and the activation energy for each of these rate constants that gave results, which were very close to the observed kinetic data and will be presented in the next section. As far as possible we tried to use the parameter values reported in various published studies. For instance, the activation energy for the initiation step (step 1) was reported by Hattori et al. [12] based on their experimental data. Both the Arrhenius parameters for the constants k_5, k_7 and k_8 were taken from the literature [8,11]. Those for k_{13} were reported by Hendry [11]. However, in their later review Hendry and Mill [8] discussed in detail the intrinsic kinetics of this bimolecular termination step (formation of the $RO^\bullet$ radicals in the solvent cage, its subsequent escape from the cage to form ROOR in competition with the so-called 'concerted' formation of alcohol and aldehyde or further chain transfer). They have also provided estimates of the rate constants for each of these intrinsic processes. Putting together all this information it was possible to assign values to the Arrhenius parameters for the overall bimolecular self-termination of the $RO_2^\bullet$ radicals that appear in Table 3. From Table 2 it can be seen that there is not much difference between the experimentally determined values reported by Hendry [11] and the ones obtained by a theoretically more consistent estimate derived in their later work [8].

Table 2
Estimated values of rate constants for the elementary reactions in cumene autoxidation from the reported Arrhenius parameters

Rate constants	Values at 120 °C (literature)
k_1	1.02 s^{-1} [12]
k_3	~1.0 × 10^9 m^3/kmol/s [8]
k_4	7.56 m^3/kmol/s [11]; 20.07 m^3/kmol/s [8]
k_5	21.20 × 10^5 m^3/kmol/s [8]
k_6	18.0 × 10^5 m^3/kmol/s [8]
k_7	8.1 × 10^5 m^3/kmol/s [11]
k_8	1.93 × 10^6 s^{-1} [8]
k_{10}	1.34 × 10^{-1} m^3/kmol/s [8]
k_{13}	9.26 × 10^4 m^3/kmol/s [11]; 6.76 × 10^4 m^3/kmol/s [8]

Table 3
Arrhenius parameters for the rate constants used in this work

Rate constants	ln A	E (kJ/mol)
k_1	23.56 s^{-1}	103.76
k_3	25.19 × 10^{-3} m^3/kmol/s	14.04
k_4	27.93 × 10^{-3} m^3/kmol/s	55.47
k_5	28.55 × 10^{-3} m^3/kmol/s	22.84
k_6	26.19 × 10^{-3} m^3/kmol/s	15.61
k_7	22.57 × 10^{-3} m^3/kmol/s	29.29
k_8	28.71 s^{-1}	46.02
k_{10}	21.82 × 10^{-3} m^3/kmol/s	42.38
k_{12}	33.58 × 10^{-3} m^3/kmol/s	33.11
k_{13}	28.16 × 10^{-3} m^3/kmol/s	33.11
k_{14}	33.56 × 10^{-3} m^3/kmol/s	33.11

For the rate constant k_6 available estimate from the literature was indirect and probably open to question. This constant, having a bearing on the DMPC/ROOR ratio in the product, was chosen to approximate the observed data and accordingly values of the Arrhenius parameters were assigned. For the hydrogen atom transfer to $RO_2^\bullet$ radicals (cumyl in step 4) Arrhenius parameters have been reported [8,11]. The oxidation of alkyl radicals forming the peroxy radicals themselves (step 3) is said to be very fast, the rate constant likely to be of the same order of magnitude as for typical exothermic radical–radical reactions with essentially no activation energy [8]. Though this is generally true, we found the need to re-estimate the parameters for both these steps (3 and 4) in order to be consistent with the observed small but finite dependence of the rate of CHP formation on the oxygen partial pressure in the case of cumene autoxidation [12,13]. As for the propagation reaction involving the methyl radicals (step 10), the reported range of values was found to be too low and needed re-estimation.

Thus, we were left with the estimation of the rate constants for the propagation steps 3, 4 and 10, namely k_3, k_4 and k_{10}, and those for the two subsidiary termination steps (k_{12} and k_{14}) apart from the frequency factor for the initiation rate constant k_1. In absence of specific information further simplification was achieved by assuming identical activation energy values for k_{12} and k_{14} as the one for k_{13}. Thus, at any temperature we estimated values for the parameters k_3, k_4, k_{10} and ratios k_{13}/k_1, k_{13}/k_{12} and k_{13}/k_{14} by trying to predict as closely as possible observed temporal profiles of concentration of cumene and CHP and the effect of the dissolved oxygen concentration on the rate of CHP production [12]. Clearly, this was a much reduced estimation

problem than the one we started with. Moreover, by virtue of this re-assessment of the reported values of the rate parameters we now had a better idea of both the guess values and the approximate range to be used for each parameter during estimation. The responses calculated by the model were used to form the deviations from the experimental data and the objective function constituted of the sum of squares of these deviations were minimized by the Marquardt-Levenberg method (IMSL module BCLSF was used in this work) for estimating these parameters. From these determinations both the Arrhenius parameters for k_3, k_4, k_{10} and the frequency factors for k_1, k_{12} and k_{14} were estimated and reported in Table 3.

4. Results and discussion

4.1. Prediction of the concentration profiles

Hattori et al. [12] presented data on the time variation of the concentrations of cumene and CHP observed in course of their experimental study of autoxidation of cumene in a semi-batch bubble column reactor. On the basis of their simplified kinetic model, based on the assumptions pointed out in Section 2, they derived approximate analytic expressions for the rates of cumene depletion (R_{RH}) and CHP production (R_{CHP}). Furthermore, they argued that the effect of oxygen partial pressure on the rates is small but not negligible. Based on their experimental observations they made a further assumption of effectively constant dissolved oxygen concentration independent of the conversion at a given level of oxygen partial pressure and the specific bubbling condition during a batch run period, while the rates were affected with the change of the set partial pressure. The final form of the rates used by the authors [12] were

$$-R_{RH} = K[RH]\sqrt{[ROOH]} + 2k_1[ROOH] \quad (17)$$

$$R_{CHP} = K[RH]\sqrt{[ROOH]} - k_1[ROOH] \quad (18)$$

The 'effective rate constant' K in the above equations was given by

$$K = \frac{p'_{O_2}k_3/H[RH]_{av}}{1 + (p'_{O_2}k_3/k_4H[RH]_{av})}\sqrt{\frac{k_1}{k_{13}}} \quad (19)$$

where p'_{O_2} denotes the partial pressure in equilibrium with the dissolved oxygen concentration and the subscript 'av' denotes an average value of [RH]. Using the measured concentration–time data the 'rate constant' K was determined. Assuming a constant K (for a specific temperature and oxygen partial pressure condition), Eqs. (17) and (18) were used by the authors [12] to back-calculate the integral cumene and CHP concentration profiles that practically traced the experimental data points (their Fig. 7).

The general dynamic model presented in this work with the rate parameters tabulated in Table 3 can be used to predict very similar concentration profiles without making any of the above assumptions. However, in order to approximate the experimental conditions of Hattori et al. [12] more exactly, we assumed a constant dissolved oxygen concentration to prevail, thus ignoring

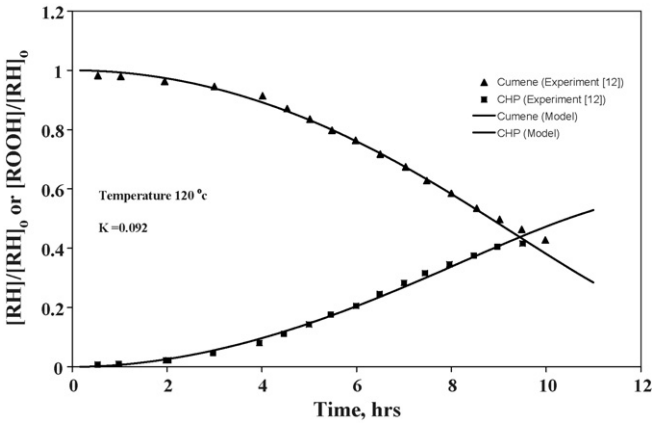

Fig. 1. Comparision of the predicted time variation of the cumene and CHP concentration with the observed profiles.

Eq. (14). The rest of the model equations were solved and the predicted cumene and CHP concentration profiles were compared in Fig. 1 with the reported observed data. It can be seen that the new model simulates the experimental data very closely indeed, including the apparent (though slight) autocatalytic increase in both the CHP production and the cumene depletion rates midway through the batch time. Under the conditions of the simulation (and using the values of the rate parameters from Table 3) the value of K calculated was 0.092 in comparison with 0.083, the value used in their paper. Considering that the model presented here is a much more general one, with independently set values for the various rate parameters, the two values of K are remarkably close. This is an indirect validation of the kinetic model and the rate parameters. As we shall presently see, the predicted variation of K with p'_{O_2} was also found to be quite consistent with the observed data.

4.2. Variation of K with p'_{O_2}

Hattori et al. [12] plotted experimentally determined values of the 'rate constant' K against p'_{O_2}. These experiments were conducted at three temperatures (namely, 110, 120 and 130 °C) and for the purpose of comparison the terminal conversion was set so as to yield a CHP concentration of 2 kmol/m^3. At a variety of preset dissolved oxygen concentrations (and hence for a series of p'_{O_2} values) the new model was used to calculate the values of K as defined by Eq. (19) and the plots of the variation of K with p'_{O_2} were generated at the three temperature levels. In the interest of easy comparison with the figures appearing in the original publications [12,13] the units of the quantities used therein were retained in Fig. 2 and the remaining figures to be discussed in this and the subsequent subsections. The predicted variation compared (see Fig. 2) very well with those observed except at very low dissolved oxygen concentrations. At such low levels the assumption underlying the derivation of the relationship is questionable. However, Fig. 2 demonstrates the small but definite dependence of the CHP production rate (or the cumene depletion rate) on the oxygen partial pressure at any temperature. As the temperature is increased from 110 to 130 °C this dependence is seen to become

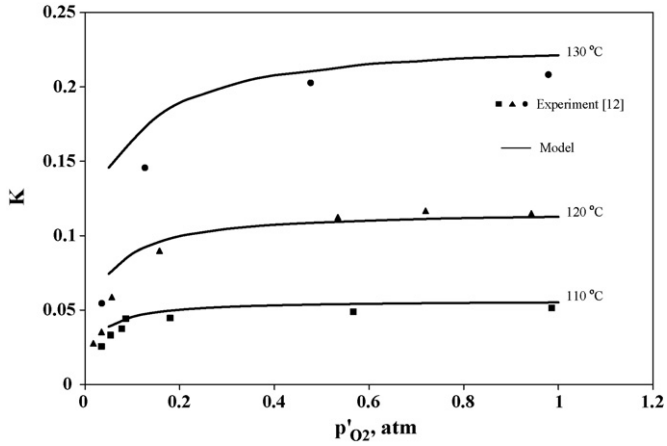

Fig. 2. Comparison of the predicted dependence of K on p'_{O_2} with the observed data.

stronger.

Hattori et al. [12] had also provided another plot of $1/K$ against $1/p'_{O_2}$, as a verification of the linear relationship between these quantities, which could be obtained by taking reciprocals of the two sides of Eq. (19). It is seen from Fig. 3 that our model also provides essentially the same relationship as appropriate at each temperature.

4.3. Dependence of the rate of CHP production on the oxygen partial pressure

In the above sub-section the oxygen dependence of the key rates that drive the oxidation process was shown in a slightly indirect manner, i.e., in the form of the dependence of an 'effective' or combined rate constant on the dissolved oxygen concentration. Though Andrigo et al. [13] essentially used the same basic rate expressions as Hattori et al. [12] the former workers identified a direct linear relationship between the rate of CHP production (neglecting the CHP depletion by initiation and other elementary processes) and the oxygen partial pressure and the cumene concentration. This relationship can be written as

$$\frac{[\mathrm{RH}]\sqrt{[\mathrm{ROOH}]}}{R_{\mathrm{CHP}}} = \frac{\sqrt{k_{13}}}{k_4\sqrt{k_1}} + \frac{H\sqrt{k_{13}}}{k_3\sqrt{k_1}}\frac{[\mathrm{RH}]}{p_{O_2}} \tag{20}$$

Andrigo et al. made their kinetic study in a 2 l CSTR with constant chosen levels of oxygen partial pressure being maintained in the overhead. Also, the reactor temperature and the liquid residence times were varied. They claimed that the reaction was essentially kinetically controlled under the conditions and using values of the measured concentrations and known oxygen partial pressure levels and the rates derived there from, the authors plotted the left hand side quantity against $[\mathrm{RH}]/p_{O_2}$ as per Eq. (20) and verified the implied linearity.

In this work focused on the kinetic model being tested in an air-sparged batch reactor the exact conditions in the above experiments would not be reproduced. However, there is every reason to anticipate, based on the model comparison with Hattori et al.'s experimental data, that a relationship such as Eq. (20) should also be possible to reproduce with the new model irrespective of the reactor one uses. We, therefore, ran the model up to a cumene conversion leading to a CHP concentration of ~2 kmol/m^3 at three temperature levels (namely, 105, 115 and 125 °C) and at various constant oxygen partial pressures. From these calculations the requisite quantities to be plotted were obtained and the results compared with the data due to Andrigo et al. [13].

It was observed, however, that though a linear relationship was clearly discernible, the slope and the intercept at each temperature level were different (the slope was more, the intercept less) than those characterizing the experimental data. After some trials, it occurred to us that this discrepancy could be easily removed by a minor adjustment in the values of only the frequency factors for the rate constants k_3 and k_4, with no change in any other rate parameters in Table 3, including the activation energies for these two propagation steps. With reference to Table 3, the $\ln A$ value for the rate constant k_3 would require to be changed to 25.78×10^{-3} and that for k_4 to 27.59×10^{-3}. Fig. 4 shows how well the model predictions (made using these modified parameters) compared with the observed quantities. The need for the minor adjustments in just these two parameters arose due to the slight differences in the oxygen partial pres-

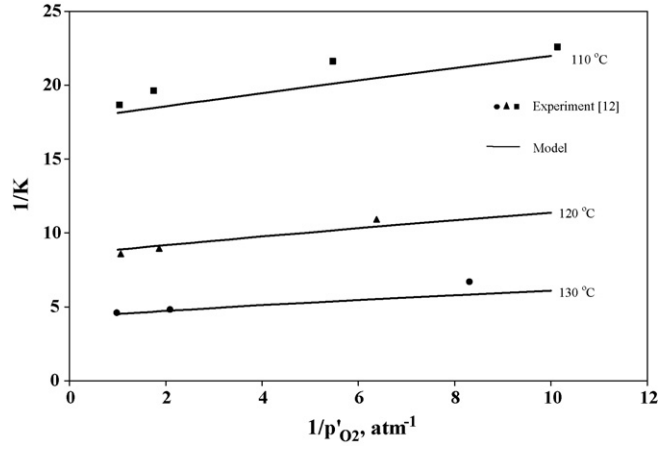

Fig. 3. Verification of the predicted linear relationship between $1/K$ and $1/p'_{O_2}$ against observed data.

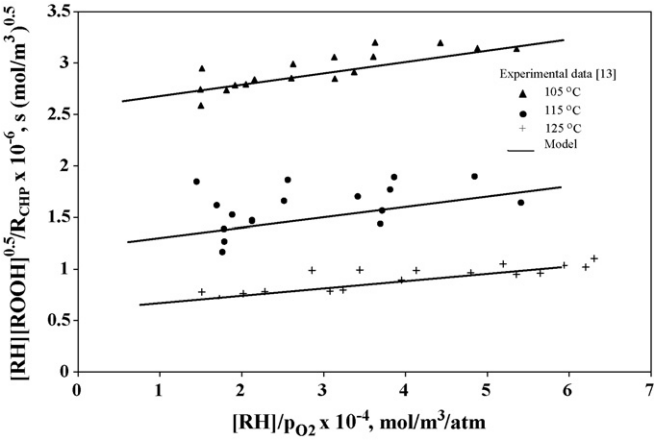

Fig. 4. Effect of oxygen partial pressure on the rate of CHP production.

sure dependence of the rates as observed independently by two groups of workers (historically apart by over 20 years) in very different reactor configurations. It only goes to show how the new general model developed here can be used to re-estimate some of the parameters of the model should it become necessary in the light of a new and reliable set of experimental data.

4.4. Selectivity relationship

As a further check on the soundness of the model, following Andrigo et al. [13] we derived the following relationship between the rates of production of the two key side products, namely, DMPC and ACP using Eq. (10), ignoring the third term as a much smaller contribution, and Eq. (11):

$$\frac{R_{\mathrm{DMPC}}}{[\mathrm{RH}] \cdot R_{\mathrm{ACP}}} = \frac{k_5}{k_8} + \frac{k_6}{k_8}\frac{[\mathrm{ROOH}]}{[\mathrm{RH}]} \tag{21}$$

From the calculated results a linear relationship between $R_{\mathrm{DMPC}}/[\mathrm{RH}]/R_{\mathrm{ACP}}$ and [ROOH]/[RH] could be obtained. Andrigo et al. [13] also made a similar plot based on their data. Both the slope and the intercept obtained by us turned out to be a little higher than those reported by these authors. Again this discrepancy could be eliminated by a little increase in the value of the frequency factor for k_8 (by about 1.6 times) and the linear plot resulting from the model predictions made with this modified parameter is shown in Fig. 5. The model now fits the experimental data (see Fig. 3 of Ref. [13]) quite well. The value of k_8 calculated from the parameters reported in Table 3 was based on published low temperature small-scale studies (under restricted conditions) conducted for elucidating the kinetics of the elementary steps constituting the overall free-radical mechanism. In the context of a direct study on cumene autoxidation under commercial operating conditions with complete product distribution as observed in a typical engineering bench scale study [13], the need for retuning some key parameters in order to be consistent with the data may arise. The fact that with a small change in just one rate parameter the model fits observed data on the product selectivity gives us hope that the model is robust and manifestly adaptable to data from disparate sources with marginal effort.

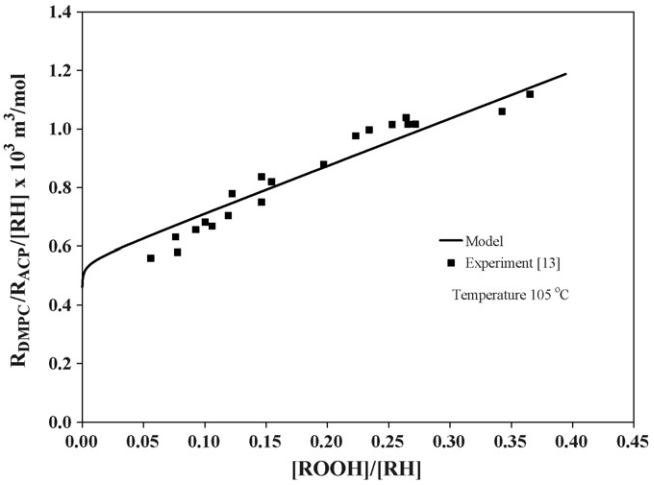

Fig. 5. Simplified selctivity relationship.

4.5. Predicted product distribution at the exit of a continuous air-sparged cumene oxidation reactor

So far we attempted to validate the new model presented here in terms of various published kinetic relationships and concentration profiles. The ultimate utility of the model lies in our ability to embed the kinetic model in an appropriate model for a continuous air-sparged reactor of the type used in commercial phenol manufacturing facilities and thereby predict the product distribution at the reactor exit. Such a reactor model, apart from the detailed and consistent kinetic model like the present one, requires appropriate representation of the flow and mixing and providing values for the gas hold-up, interfacial area and the liquid phase mass transfer coefficient for the specified sparging and/or agitation device configuration. This could be done preferably by experimental cold flow studies, such as the one conducted by Andrigo et al. [13] on the specific reactor used, or in the absence of experimental data, by using appropriate published correlations for the said hydrodynamic and transport parameters [23–26] or by the use of computational fluid dynamic modeling tools [27]. Despite well-known and sometimes justifiable reservations against the use of generalized correlations, the advantage of obtaining a quick and practical estimate of these parameters cannot be overemphasized. The primary emphasis of this paper is on placing a sound kinetic model for the autoxidation of cumene in public domain. Before signing off we would like to quickly see how a simply constructed continuous air-sparged cumene oxidator model could make a priori predictions of the exit liquid composition under typical commercial operating conditions.

In a recently published paper [28], we have presented the basic model equations for a continuous air-sparged reactor stage for cyclohexane oxidation. The reactor model for cumene oxidation was built using this scaffolding, with the gas and the liquid phase equations remaining essentially the same, except that in the liquid phase we now have five product components (CHP, DMPC, ACP, ROOR and RR) apart from cumene and the dissolved oxygen.

The gas hold-up, interfacial area and the liquid phase mass transfer coefficient were calculated by using the Akita–Yoshida correlations [22] in order to be consistent with the parameter values used in the batch reactor calculations presented earlier and the same physicochemical properties were used. The same set of correlations was also used by Krzysztoforski et al. [29] in their simulation of an industrial scale multi-stage cyclohexane oxidation reactor. This, however, is not to be taken as a recommendation in favour of these correlations as against several others reported in the literature, which could also be tried out for a specific design/simulation job.

The kinetic sub-model, which supplies the values for the rates of depletion/generation of these seven species concentration, was based on Eqs. (7) through (13) along with the ancillary equations for determining the pertinent free-radical concentra-

Table 4
Comparison of the predicted liquid composition at the exit of a single air-sparged continuous cumene oxidation reactor vis-à-vis reported test run data for a typical commercial reactor configuration

Components	Simulation (wt%)		Test run data [13] (wt%)	Simulation (wt%)		Test run data [13] (wt%)	Simulation (wt%)		Test run data [13] (wt%)
	This work	Andrigo et al. [13]		This work	Andrigo et al. [13]		This work	Andrigo et al. [13]	
Cumene	74.90	72.3	74.9	72.44	69.9	72.4	69.29	67.5	69.3
CHP	19.06	20.1	17.9	20.57	22.4	20.2	22.45	24.5	23.0
DMPC	2.26	2.11	1.88	2.62	2.28	2.06	3.10	2.46	2.27
ACP	0.34	0.48	0.4	0.39	0.51	0.43	0.46	0.55	0.47
ROOR	0.25	0.053	0.044	0.30	0.061	0.05	0.37	0.068	0.058

Note: The complement to 100% is due to inert hydrocarbons.

tions. The complete set of non-linear algebraic equations was solved by Newton–Rhapson method.

The simulations were done assuming a 0.025 m^3 reactor volume and the reactor temperature set at 115 °C, superficial air velocity 0.15 m/s, oxygen partial pressure 0.021 MPa. At this level of air flow rate this variable has little effect on the conversion and/or selectivity. The latter were primarily affected by the variation in the liquid flow rates so as to give mean residence times in the range 25,000–30,000 s. This could represent a pilot plant scale cumene oxidation reactor under realistic operating conditions.

The liquid compositions were calculated at three conversion levels in the range of interest using the original set of parameters from Table 3. Andrigo et al. [13] provided several sets of test run data (their Table 1) on the liquid composition at the exit of a number of reactors of different size forming a part of one of the EniChem ANIC industrial production lines in their phenol manufacturing plant in Italy. We have chosen three test run data sets at varying cumene conversion values and compared (see Table 4) the predicted and the observed liquid composition. In the same table, we have also included for easy comparison the liquid composition obtained by the same authors [13] using their more elaborate reactor simulation model.

The point to note from this table is that our model has predicted the liquid composition at each of the conversion levels closely vis-à-vis the test run data in terms of the cumene, CHP, DMPC and ACP contents. The model predictions based on our model were at least as good as and in some cases better than the ones made by the more sophisticated model [13]. In the case of ROOR, though in terms of the wt% composition there is considerable over-prediction, the molar ratio of DMPC to ROOR was found to be at ∼20, which was in the range said to be maintained in the experimental 21 CSTR data [13]. Indeed this observation was borne in mind during our parameter estimation. If, however, as seen in the test run data from the commercial reactor, the oxidate is consistently leaner in ROOR, a further readjustment in some of the termination rate constants, notably k_{13} and/or k_{12} may be required. But this should be done only in the event of a systematic and detailed study in a particular experimental/plant facility demonstrating a need for retuning.

4.6. Effect of process and operating variables on the product distribution at the exit of an air-sparged cumene oxidation reactor network

In practice [4], several air-sparged oxidation reactors are connected in series, with the effluent liquid stream from one flowing into the next while identical air stream, distributed evenly among all the reactor stages, is blown into each of them at the bottom using a suitable sparging device. It is a simple matter to extend the single reactor model discussed above to that of a multi-stage reactor network with, if necessary, resetting pressure, temperature and air composition at each stage. While it would be beside the scope of this paper to attempt simulating any particular commercial configurartion, we believe that the following discussion would bring out interesting observations regarding the process and operating variables that may possibly be used to influence the product distribution at the exit of the reactor system.

Before turning to the multi-stage system, let us briefly illustrate how, for the given kinetics, mass transfer effect might come

Table 5
Effect of staging, air rate and temperature on the product distribution in an air-sparged continuous cumene oxidation reactor system

Case	N_R	u_g (m/s)	Temperature (°C)	Cumulative residence time (h)	Components					
					Cumene (wt%)	CHP (wt%)	DMPC (wt%)	ACP (wt%)	ROOR (wt%)	RR (wt%)
1	1	0.15	113	2.07	75.37	22.68	0.69	0.09	1.08	0.06
2	1	0.1	113	2.10	75.58	22.47	0.69	0.09	1.04	0.10
3	1	0.075	113	2.20	75.62	22.37	0.72	0.10	0.99	0.19
4	1	0.05	113	2.68	75.64	22.02	0.86	0.12	0.80	0.56
5	1	0.0375	113	3.36	75.58	21.59	1.05	0.14	0.63	1.00
6	1	0.025	113	4.79	75.60	20.60	1.42	0.20	0.43	1.75
7	4	0.025	113/113/113/113	5.09	75.47	21.87	1.01	0.14	0.36	1.16
8	4	0.025	113/109/105/103	5.33	75.66	22.66	0.62	0.08	0.53	0.46

into play and thereby adversely affect the product distribution. With reference to the first six cases of model predicted results in Table 5, all of which used a single reactor, the only variable was the air flow rate, at a constant pressure of 0.64 MPa and a temperature of 113 °C. As the superficial air velocity was reduced from 0.15 to 0.025 m/s, almost identical cumene conversion (∼25%) was achieved at increasingly longer residence times, thus indicating a progressively increasing influence of mass transfer. More strikingly, at the same time the CHP selectivity also suffered, with a gradual increase in the side product (DMPC, ACP) concentrations. That staging the process (using a multi-stage configuration of four reactors in series) would counteract on the loss in selectivity to an extent was expected. Thus, in the case no. 7 where identical pressure and temperature were used in all the four stages and the lowest air rate was maintained, there is a clear improvement in the CHP selectivity. More interestingly, as the temperature at each stage was progressively lowered (see case 8, with 113 °C in the stage 1 and 103 °C at the stage 4, with identical pressure, these conditions being the same as shown on the example flowsheet for a large scale cumene oxidation process [4]) the CHP selectivity was brought back almost to the level of case 1 (indeed a little better than that) which used a much higher air flow rate.

These results of a simulation study may not be taken too literally as this is based on a simple reactor model. However, this shows that practical conclusions of use to the process engineers may be derived by combining the basic kinetic model presented in this work with a more rigorous reactor model with an appropriate fluid dynamic description.

5. Conclusions

In the foregoing we have shown that it is possible to formulate a consistent free-radical mechanism for cumene autoxidation, comprising of most of the elementary steps known to play important roles in controlling the rates and product selectivity. Based on the kinetic analysis of the resulting reaction network, individual component rates (net consumption/production) could be derived. This formulation uses an important cross-termination step replacing an often used but less likely one and the treatment avoided a couple of time-honored assumptions about the relationship and values of the rate constants for the termination steps. By referring to the existing body of research on the uncatalyzed free-radicals mediated major elementary reactions such as radical initiation, propagation, the chain transfer and termination we could identify and/or re-estimate values for all the pertinent kinetic parameters that gave rates of overall cumene depletion, oxygen consumption and the CHP production broadly in conformity with the observations reported in the literature. We were actually able to reproduce quite well a set of well-regarded published data of long standing on cumene and CHP concentration profiles and the effect of oxygen partial pressure on the rates in a batch reactor. It was a measure of success of the new kinetic model that on embedding the same within a simple reaction engineering model for a single air-sparged continuous cumene oxidator of the type used in commercial installations, the liquid oxidate composition at the reactor exit could be predicted that compared closely with some limited published data from an industrial reactor. Finally, interesting conclusions could be derived from a simulation study of a multiple oxidators-in-series network, regarding the effect of staging, stage temperature and the air rate on the hydroperoxide selectivity and the side product distribution in the oxidate.

The model presented in the paper should be a useful tool in the analysis and design of cumene oxidation reactors. With minor adaptations and re-estimation of some of the parameters it should be possible to use the same to simulate other autoxidation reactors as well.

References

[1] J.B. Saunby, B.W. Kiff, Liquid-phase oxidation—hydrocarbons to petrochemicals, Hydrocarbon Process. 55 (1976) 247–252.
[2] J.E. Lyons, Up petrochemical value by liquid phase catalytic oxidation, Hydrocarbon Process. 59 (1980) 107–119.
[3] A.K. Suresh, M.M. Sharma, T. Shridhar, Engineering aspects of industrial liquid-phase air oxidation of hydrocarbons, Ind. Eng. Chem. Res. 39 (2000) 3958–3997.
[4] M.K. Guerra, Process Economic Program Report No. 22C (Phenol Supplement C), SRI International, California, March 1991.
[5] N.M. Emanuel, E.T. Denisov, Z.K. Maizus, Liquid-Phase Oxidation of Hydrocarbons, Plenum Press, New York, 1967.
[6] J.A. Howard, Homogeneous liquid phase autoxidations, in: J.K. Kochi, J.A. Olah (Eds.), Free Radicals, vol. I, John Wiley and Sons, New York, 1973, pp. 3–62.
[7] G. Franz, R.A. Sheldon, Oxidation, in: B. Elvers, S. Hawkins, G. Shultz (Eds.), Oxidation, Ullmann Encyclopedia of Industrial Chemistry, vol. A18, VCH Verlagsgesellschaft, Weinheim, 1991, pp. 271–285.
[8] T. Mill, D.G. Hendry, Kinetics and mechanisms of free radical oxidation of alkanes and olefins in the liquid phase, in: C.H. Bamford, C.F.H. Tipper (Eds.), Comprehensive Chemical Kinetics, vol. 16, Elsevier, Amsterdam, 1980, pp. 1–87.
[9] N.M. Emanuel, G.E. Zaikov, Z.K. Maizus, Oxidation of Organic Compounds: Medium Effects in Radical Reaction, Pergamon Press, Oxford, UK, 1984, pp. 6–73.
[10] T.G. Traylor, C.A. Russell, Mechanisms of autoxidation. Terminating radicals in cumene autoxidation, J. Am. Chem. Soc. 87 (1965) 3698–3706.
[11] D.G. Hendry, Rate constants for oxidation of cumene, J. Am. Chem. Soc. 89 (1967) 5433–5438.
[12] K. Hattori, Y. Tanaka, H. Suzuki, T. Ikawa, H. Kubota, Kinetics of liquid phase oxidation of cumene in bubble column, J. Chem. Eng. Japan 3 (1970) 72–78.
[13] P. Andrigo, A. Caimi, P. Cavalieri d'Oro, A. Fait, L. Roberti, M. Tampieri, V. Tartari, Phenol–acetone process: cumene oxidation kinetics and industrial plant simulation, Chem. Eng. Sci. 47 (1992) 2511–2516.
[14] P.L. Mills, R.V. Chaudhari, Reaction engineering of emerging oxidation processes, Catal. Today 48 (1999) 17–29.
[15] A.K. Roby, J.P. Kingsley, Oxide safely with pure oxygen, CHEMTECH 26 (1996) 39–46.
[16] A.K. Suresh, T. Shridhar, O.E. Potter, Autocatalytic oxidation of cyclohexane—modeling reaction kinetics, AIChE J. 34 (1988) 69–80.
[17] R. Pohorecki, J. Baldyga, W. Moniuk, W. Podgorskya, A. Zdrojkowski, P.T. Wierzchowski, Kinetic model of cyclohexane oxidation, Chem. Eng. Sci. 56 (2001) 1285–1291.
[18] A. Bhattacharya, A. Mungikar, Kinetic modeling of liquid phase oxidation of cyclohexane, Can. J. Chem. Eng. 81 (2003) 220–229.
[19] S.M. Mahajani, M.M. Sharma, T. Shridhar, Uncatalysed oxidation of cyclohexene, Chem. Eng. Sci. 54 (1999) 3967–3976.
[20] S.S. Mahajan, M.M. Sharma, T. Shridhar, Uncatalysed liquid phase oxidation of cyclododecene with molecular oxygen, Ind. Eng. Chem. Res. 43 (2004) 3289–3296.

[21] D.I.R. Low, The unsteady state absorption of oxygen in cumene, Can. J. Chem. Eng. 45 (1967) 166–170.
[22] K. Akita, F. Yoshida, Bubble size, interfacial area and mass transfer coefficient in bubble columns, Ind. Eng. Chem. Proc. Des. Dev. 13 (1974) 84–91.
[23] P.V. Danckwerts, Gas–Liquid Reactions, McGraw-Hill Book Company, New York, 1970.
[24] H. Van Landgehm, Multiphase reactors: mass transfer and modeling, Chem. Eng. Sci. 35 (1980) 1912–1949.
[25] J.-C. Charpentier, Mass transfer rates in gas–liquid absorbers and reactors, in: T.B. Drew, G.R. Cocklet, J.W. Hoopes Jr., T. Vermeulen (Eds.), Advances in Chemical Engineering, vol. 11, Academic Press, New York, 1981.
[26] S.-Y. Lee, Y.P. Tsui, Succeed at gas–liquid contacting, Chem. Eng. Prog. 95 (1999) 23–49.
[27] V.V. Ranade, Computational Flow Modeling for Chemical Reactor Engineering, Academic Press, London, 2002.
[28] A. Bhattacharya, Modeling a continuous multistage liquid phase cyclohexane oxidation reactor network, Chem. Eng. Proc. 44 (2005) 567–579.
[29] A. Krzysztoforski, Z. Wojcik, R. Pohorecki, J. Baldigya, Industrial contribution to the reaction engineering of cyclohexane oxidation, Ind. Eng. Chem. Proc. Des. Dev. 13 (1974) 84–91.